

Quality factor scaling of resonances related to bound states in the continuum

Aleksandra A. Kutuzova ¹ and Mikhail V. Rybin ^{1,2}¹*ITMO University, School of Physics and Engineering, St. Petersburg 197101, Russia*²*Ioffe Institute, St. Petersburg 194021, Russia* (Received 31 October 2022; revised 19 April 2023; accepted 20 April 2023; published 5 May 2023)

In real samples, bound states in the continuum (BICs) are manifested as resonances with a finite, although significantly high, quality (Q) factor. Control over the Q factor through an asymmetry parameter (i.e., an intentional defect of the structure, allowing structural imperfections to be introduced on purpose) allows tailoring the coupling strength with the modes of the free space. In most systems, Q has an inverse quadratic dependence on the asymmetry parameter. However, various applications require different scaling laws. For instance, sensors require a steeper dependence, whereas light generation needs a less steep one for robustness. Here, we consider a metasurface consisting of dielectric rods with air holes inside of them, obtaining several different scaling laws. Our analysis reveals that BIC has dominant and asymmetry-induced multipole terms. Depending on the radiation properties of the induced multipoles and their amplitude in the case of vanishing asymmetry, the exponent in the scaling law lies in the range from -4 to -1.75 , including the common case of -2 .

DOI: [10.1103/PhysRevB.107.195108](https://doi.org/10.1103/PhysRevB.107.195108)

I. INTRODUCTION

Bound states in the continuum (BICs) were discovered a century ago in quantum mechanics [1], although they are a general phenomenon related to destructive interference occurring due to wave nature [2]. Over the last decade, they have attracted significant interest after the shift to optics [3–6]. Unlike electrons, the photon energy always lies in the continuum, and light trapping is a challenging fundamental problem. A solution to this problem promises many opportunities for various applications, and BICs can be considered as a way to engineer a perfect resonator with an infinite quality (Q) factor. However, reality permits no unlimited singularities. To begin with, a perfect BIC requires an infinite length sample; further, inevitable fabrication roughness and material absorption spoil the ideal destructive interference condition. Moreover, a perfect BIC decoupled from the continuum is useless, since it does not interact with other waves. In real samples, BICs manifest themselves as supercavity modes, the so-called quasi-BICs, which are inherently noninfinite, but have high values of the Q factor [7].

High- Q BIC-related resonances are used to enhance light-matter interactions [8,9]. Among other applications, laser [10–16] and harmonic generation [17–21] and sensing [22–26] were reported. For the former, the resonator Q -factor dependence on imperfections should be weak to improve robustness, while for the latter, it should be strong to increase the sensibility. Thus, for different applications, different dependences are needed.

The Q factor has a cubic and even higher-order dependence on the sample size [27–29]; however, this property is hard to use, as an electromagnetic field radiates at the boundaries of the structure, in contrast to the asymmetry-related radiation in the normal direction, which is much more suitable for practical applications of BIC [10,22]. Recently, fourth- or even sixth-order power laws were predicted for two or even three

BICs merged in a many-parameter space [30]. Koshelev *et al.* derived a formula for the Q factor as an inverse quadratic function of an asymmetry parameter and demonstrated that systems with symmetry-protected BICs do obey this scaling law [31]. However, to the best of our knowledge, reports on exponent values below 2 are lacking.

Here, we study a high-symmetry system that allows us to remove symmetry elements independently. The system comprises cylindrical rods supporting Mie-type modes that facilitate the theoretical analysis of the system. We show that the Q factor scaling law is not restricted by the reported dependence $Q \propto \alpha^{-2}$, where α is an asymmetry parameter, but other values of the exponent are possible as well. We carry out a multipole decomposition analysis, which reveals two multipole contributions to the supercavity mode: a dominant one and one induced due to the asymmetry of the system. The scaling behavior of the Q factor is governed by the interplay of the dominant and induced contributions. Such a simple toy model reveals the underlying physics, which is useful for the further design of devices.

II. RESULTS

Figure 1 shows a metasurface consisting of parallel rods, the lattice constant a , rod radius $R = 0.25a$, and permittivity $\epsilon = 12$. Each cylinder has a small round hole with a radius $r = 0.2R$. We study transverse electric (TE)-polarized waves (the magnetic field oscillates along the rod axis). The symmetry elements are translational symmetry T_a , and mirror symmetries σ_{x1} , σ_{x2} , and σ_y , which correspond to the y and x coordinates, respectively. For σ_{x1} , the mirror plane is located in the middle between neighboring rods, and for σ_{x2} , the plane passes through the rod center.

We simulated the metasurface photonic band structure with COMSOL (Fig. 2). We consider a subwavelength regime below the second-order light cones with two eigenmodes, mode 1

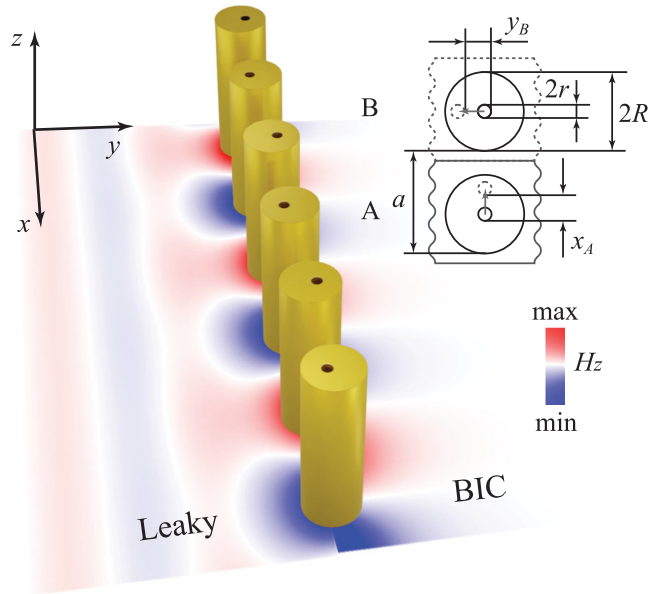


FIG. 1. Schematic view of the metasurface supporting different regimes of radiation leakage rate. Inset: Doubled unit cell composed of a pair of rods labeled A and B. In each rod, the air hole is displaced from the center.

and mode 2. Both modes are guided, since they lie below the light line. The low-frequency mode 1 has a dipolelike distribution of the magnetic field, and the high-frequency mode 2 has a quadrupolelike profile. The fields of neighboring rods have opposite phases, according to the wave vector at the Brillouin zone edge π/a . Note that the profile of mode 1 is an odd

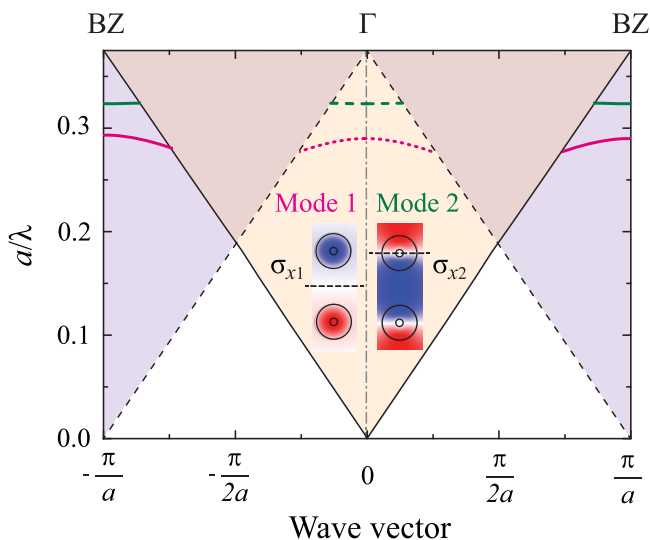


FIG. 2. Photonic band structure of the metasurface. Solid curves show eigenmodes of the initial structure with no hole displacement (doubling with a single unit cell). The area above the light cone (shown with solid lines) is shaded. For the double-unit-cell metasurface, dashed curves and lines appear due to the different offsets of the holes in the A and B rods. The insets show the profiles of modes 1 and 2. The intensity of color indicates the magnetic field amplitude (red for positive, blue for negative).

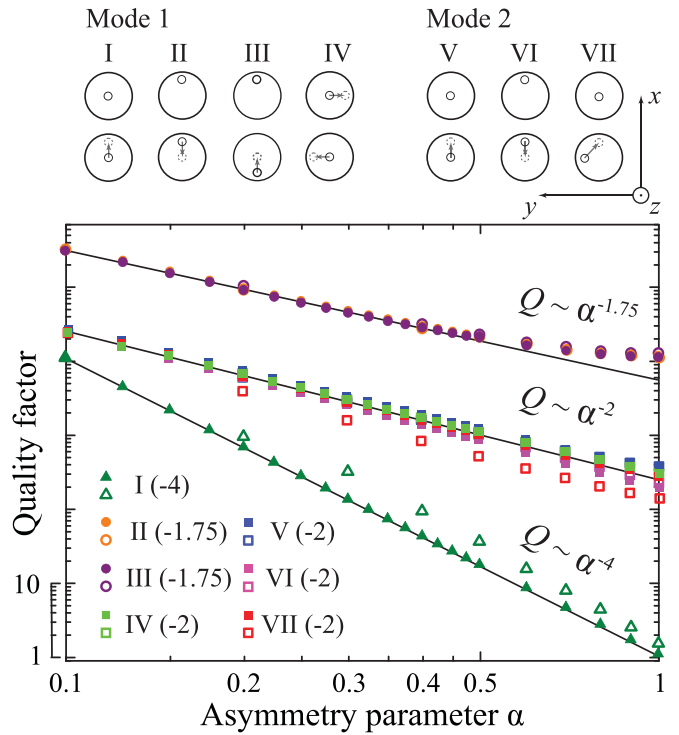


FIG. 3. Scaling of the Q factor with the asymmetry parameter for seven configurations shown schematically at the top. Solid symbols are the values obtained from complex eigenfrequencies simulated with COMSOL, and solid lines are fitting. Open symbols indicate the values obtained from the value of the Poynting vector of the outgoing wave evaluated by the multipole analysis. For each displacement configuration, the Q factor dependence is shifted along the vertical axis so that dependences with the same exponent start at the same Q value.

function with respect to σ_{x1} , and the profile of mode 2 is an even one; these modes also have opposite parities with respect to σ_{x2} . Further, we consider modes at the Γ point, having the highest symmetry.

Now, we study the hole displacement that can break each of the symmetry elements listed above. To reduce the translational symmetry, we choose a new unit cell, comprising two rods, A and B, with holes independently shifted by a vector $(x_{A,B}, y_{A,B})$ away from the rod centers (see the inset in Fig. 1). Due to this period doubling, the Brillouin zone shrinks by a factor 2, down to the interval $[-\pi/2a \dots \pi/2a]$, and additional light cones appear, with the origin at $\pm\pi/a$. Modes 1 and 2 are duplicated in the center of the Brillouin zone above the initial light cone, thus they are no longer guided. However, they might be symmetry-protected BICs. In some respects, a guided mode can be considered a BIC protected by translational symmetry. In this case, when the symmetry is broken, typical supercavity mode behavior [7] will be observed.

We collect seven displacement configurations that differ by the initial and final positions of the holes, illustrated in Fig. 3. This set covers all the possible combinations of reductions of the symmetry elements in the metasurface [32]. Each small hole is treated as a perturbation to the system. In particular,

the mode eigenfrequency is negligibly shifted, and the Q factor becomes finite. We aim to analyze the dependence of the Q factor on the hole displacements. As a dimensionless parameter of asymmetry α , we choose the hole displacement value normalized to the rod radius.

Figure 3 shows different scaling laws between the Q factor and the asymmetry parameter (the hole displacement), revealing that different configurations correspond to their own values of the exponent. Four of the seven configurations demonstrate an exponent value of -2 , which matches the law $Q \propto \alpha^{-2}$ often reported in the literature [31]. Surprisingly, one configuration shows the exponent -4 , describing a faster degradation of the BIC, and there are also configurations corresponding to a less than two power law $Q \propto \alpha^{-1.75}$ with a lower slope of the curve. We notice that if one takes into account the four-mode effective Hamiltonian corresponding to the quartic equation (see below) the value 1.75 can be written in fractional form as $7/4$, however, it is likely just a coincidence, so we use the decimal form.

Let us illustrate the three possible Q factor dependences, using representative displacement configurations. First, for the exponent value -2 , we consider the quadrupole mode 2: In the initial state, both holes are at the centers of the rods, and then the hole in rod A is shifted along the y axis (configuration V). In the initial state, there are all the symmetry elements described above, and the displacement keeps σ_y only. Thus, initially, mode 2 is a guided mode under the light cone, symmetry protected by σ_{x1} . The hole displacement reduces both symmetries responsible for the electromagnetic field confinement. Unlike the other dependences, $Q \propto \alpha^{-2}$ is common, and it is not restricted to the quadrupole-type mode 2.

Second, configuration I exhibits $Q \propto \alpha^{-4}$ scaling for the same displacement configuration V, but for the dipole-type mode 1. Despite the same symmetry breaking, the exponent is twice as large compared to that of mode 2. Finally, an exponent of -1.75 is observed for mode 1. We consider configuration II as an example: In the initial state, both holes are equally shifted from the rod center along the y axis, so the translational symmetry T_a is preserved, and σ_{x1} and σ_{x2} are broken. In this case, initially, mode 1 is a guided mode, and the displacement reduces only one element of the metasurface symmetry group. However, exactly the same Q factor dependence is observed for configuration III, with the holes shifted in opposite directions in the initial state, so that the structure has no T_a symmetry, but has σ_{x1} instead. This mode is a BIC protected by the mirror symmetry.

For analysis, we apply the multipole expansion technique [33]. The eigenmodes are normalized by the electromagnetic energy of the induced fields, estimated as $\int d\mathbf{r}[\varepsilon(\mathbf{r}) - 1] \cdot |\mathbf{E}|^2$. The field outside the rod is expanded over the outgoing waves described by the Hankel functions and the incident waves described by the Bessel functions with no singularities at the origin. We study the lowest dipolar and quadrupolar terms of the outgoing waves, since they are radiated from the mode supported by the rod. The contribution of the higher-order multipoles is negligible. The Poynting vector evaluated from the interference of the multipoles depends on the asymmetry parameter almost as much as the Q factor does, which proves the applicability of our approach.

Figure 4 shows the multipole amplitudes of rods A and B for three considered configurations. For the exponent -2 , initially, mode 2 is a quadrupole with no dipole components in the rods [Fig. 4(a)]. Note that in all the considered configurations, there is a multipole that dominates for any value of the asymmetry parameter, and another multipole has a smaller amplitude, which we refer to as the induced one. The quadrupole lobes are oriented along the x axis, which leads to zero radiation in the y direction (we consider the modes at the Γ point). In the subwavelength regime, radiation to any other direction is prohibited by the lattice arrangement of the rods, thus the quadrupoles take no part in the radiative leakage. Increasing displacement results in increasing dipole amplitudes of the rods; moreover, for the dipole mode of rod B with a nondisplaced hole, the effect is even stronger. Although the dipoles oscillate out of phase, their radiation is not mutually canceled in the far-field zone because of the amplitude mismatch. The same hole displacement results in a $Q \propto \alpha^{-4}$ scaling for mode 1. In the initial state, the excitation in each rod is described by a dipole term only [Fig. 4(b)]. As the asymmetry parameter increases, the quadrupole contribution grows linearly. Similar to the case of mode 2, the induced amplitude becomes weaker in rod A with perturbation. Besides, the amplitudes of the dominant dipole modes of different rods split, and as a result, the amplitude mismatch allows radiative leakage.

Figure 4(c) shows the multipole amplitudes for the exponent value -1.75 . Initially, the holes in both rods are displaced. Here, two terms contribute to the mode: the dominant dipole and induced quadrupole. An increase of the asymmetry parameter corresponds to a decreasing hole displacement in rod A. As a result, the induced quadrupole amplitudes decrease almost linearly. The quadrupole amplitude in the opposite rod B decreases more strongly than in the other cases. Moreover, the dipole amplitudes become slightly different, which leads to a Q -factor decrease.

To analyze the differences in the Q -factor dependences on the asymmetry parameter, we use the multipole approach. At the Γ point, each unit cell comprising two rods has the same multipole amplitudes: two for dipoles and two for quadrupoles. We notice that the dipole-quadrupole interaction between different rods is forbidden due to the parity mismatch. Thus, the model considers dipole-dipole κ and quadrupole-quadrupole ξ couplings between rods and a dipole-quadrupole coupling $\chi_{A,B}$ within each rod, which is assumed to be linear in the asymmetry parameter α (hole displacement).

First, we make a simplified assessment of the multipole interaction in the system. The case of exponent -2 is usually considered within the perturbation theory. Indeed, a linear change of the dipole-quadrupole coupling χ_A leads to a linear growth of the dipole mode in rod A, which exchanges its energy with the dipole term in rod B. Thus, for a small displacement, the difference between the dipole amplitudes in different rods grows linearly too. As a result, the amplitude of the radiated wave also grows linearly, and the Poynting vector has a quadratic dependence on α .

Mode 1 with the dependence $Q \propto \alpha^{-4}$ can be treated similarly, but in this case, there is an underlying two-step process. Linear dipole-quadrupole coupling causes quadrupole

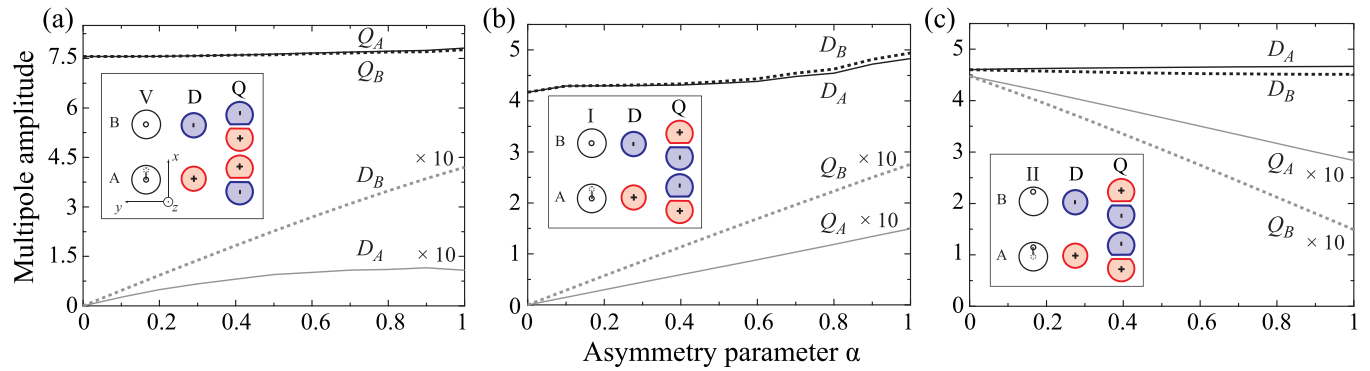


FIG. 4. Dipole and quadrupole amplitudes vs asymmetry parameter. Displacement configurations (a) V, (b) I, and (c) II demonstrate $Q \propto \alpha^{-2}$, α^{-4} , and $\alpha^{-1.75}$ scaling laws, respectively. Insets: Schemes of the hole displacement with the corresponding dipole and quadrupole phases. In all panels, dominant/induced multipole amplitudes are shown in black/gray; solid curves are for rod A, and dashed curves are for rod B. The amplitudes of induced multipoles are scaled by a factor of 10.

amplitudes to grow linearly; these quadrupoles do not radiate, as their lobes are oriented along the x axis. In turn, the quadrupole affects the amplitude of the dipole according to the linear law as well. Consequently, the total backaction effect on the dipole terms, which radiate to the far zone, provides their quadratic dependence. Thus, here we consider the leakage as a second-order process.

The exponent 1.75 cannot be described with a similar perturbation theory. For simplicity, we assume the quadrupole amplitudes in both rods to have the same dependence $Q_{A,B}(1 - \alpha)$, and the dipole-quadrupole coupling coefficients are $\chi_A = \chi_{A,B}$ and $\chi_B = \chi_{A,B}(1 - \alpha)$. We evaluate the change in the dipole amplitude as a product of the quadrupole amplitude and the coupling coefficient. Thus, the difference between the dipoles in rods A and B is a subquadratic function $\chi_{A,B}Q_{A,B}(\alpha - \alpha^2)$, which leads to a subquadratic dependence of the radiation flow.

To verify that the exponent values -1.75 , -2 , and -4 are permitted, we consider an effective Hamiltonian, a 4×4 matrix defining a four-dimensional eigenvector of the dipole and quadrupole amplitudes in two rods,

$$\hat{H}_{\text{eff}} = \begin{pmatrix} \omega_d & \kappa & \chi_A & 0 \\ \kappa & \omega_d & 0 & \chi_B \\ \chi_A & 0 & \omega_q & \xi \\ 0 & \chi_B & \xi & \omega_q \end{pmatrix}. \quad (1)$$

We use phenomenological coupling coefficients that qualitatively describe the multipole amplitudes obtained numerically for all seven configurations [32]. Then, the eigenproblem is reduced to a fourth-order equation. The obtained eigenvector is normalized to the dominant multipole amplitude in rod A, retrieved from the numerical simulations for the same parameter α . The amplitude of the radiation field depends linearly on the difference between the dipoles in two rods. That allows us to assess the dependence of the Poynting vector of the leakage radiation on the asymmetry, which for small values of α obeys power laws with indices 1.75, 2, and 4.

III. DISCUSSION AND CONCLUSIONS

Indeed, we have found that the Q -factor dependence on the asymmetry parameter can obey a power law with an exponent

of -4 and even below two -1.75 values, in addition to the common exponent -2 . The main reason for this variety is that the structure supports several multipoles decoupled from the free-space continuum (see Table I). Among these multipoles, we select the dominant one, while the other multipoles with smaller amplitudes are the induced ones. These modes stem from the high symmetry of the system in the initial state. A perturbation removes one or several symmetry elements, leading to coupling between the multipoles. What matters is that the asymmetry parameter enables an interaction with a nonradiative mode, which, in our case, is a quadrupole, and the energy leakage to the free-space modes involves a two-step process. In the common case, when induced multipoles are coupled to the free space, there is a single-step process, resulting in an exponent of -2 . If there is no excitation of the induced multipoles in the initial state, an effective two-step process appears, and each step has the amplitude efficiency linear in α , which results in a fourth-order law for the energy leakage. However, when the initial state supports an essential amplitude of the induced multipole contribution, a more complicated process occurs, and the energy interchange between the multipoles is strongly affected by the initial multipole phase. As a result, a less than two exponent -1.75 is observed.

We have considered circular rods, which allowed us to analyze the problem using a multipole-based approach and reveal the complex mechanisms governing the system's response to the variation of the asymmetry parameter. Our simple initial system is convenient for multipole calculations; in real sample fabrication, the shape of the rods can be changed to obtain an exponent value approximately in the range of $[-4 \dots -1.75]$. Another possible realization is a high-symmetry metasurface with a large number of representations, supporting counterparts of the dominant and induced modes in our system.

TABLE I. Q -factor scaling laws depending on the induced multipoles.

Zero amplitude in the initial state	Yes	Yes	No
Radiates to free space	Yes	No	No
Scaling law	$Q \propto \alpha^{-2}$	α^{-4}	$\alpha^{-1.75}$

We anticipate that our results (summarized in Table I) will pave the way for the design of photonic structures with application-tailored dependence of the Q factor on an asymmetry parameter, with exponent values either larger or smaller than the common quadratic law implies.

ACKNOWLEDGMENTS

We thank Alexey Dmitriev and Andrey Bogdanov for fruitful discussions. This work was supported by the Russian Science Foundation (21-19-00677).

-
- [1] J. von Neumann and E. P. Wigner, *Phys. Z.* **30**, 465 (1929).
- [2] C. W. Hsu, B. Zhen, A. D. Stone, J. D. Joannopoulos, and M. Soljačić, *Nat. Rev. Mater.* **1**, 16048 (2016).
- [3] D. C. Marinica, A. G. Borisov, and S. V. Shabanov, *Phys. Rev. Lett.* **100**, 183902 (2008).
- [4] E. N. Bulgakov and A. F. Sadreev, *Phys. Rev. B* **78**, 075105 (2008).
- [5] Y. Plotnik, O. Peleg, F. Dreisow, M. Heinrich, S. Nolte, A. Szameit, and M. Segev, *Phys. Rev. Lett.* **107**, 183901 (2011).
- [6] C. W. Hsu, B. Zhen, J. Lee, S.-L. Chua, S. G. Johnson, J. D. Joannopoulos, and M. Soljačić, *Nature (London)* **499**, 188 (2013).
- [7] M. Rybin and Y. Kivshar, *Nature (London)* **541**, 164 (2017).
- [8] K. Koshelev, A. Bogdanov, and Y. Kivshar, *Sci. Bull.* **64**, 836 (2019).
- [9] A. F. Sadreev, *Rep. Prog. Phys.* **84**, 055901 (2021).
- [10] K. Hirose, Y. Liang, Y. Kurosaka, A. Watanabe, T. Sugiyama, and S. Noda, *Nat. Photonics* **8**, 406 (2014).
- [11] A. Kodigala, T. Lepetit, Q. Gu, B. Bahari, Y. Fainman, and B. Kanté, *Nature (London)* **541**, 196 (2017).
- [12] M. Wu, S. T. Ha, S. Shendre, E. G. Durmusoglu, W.-K. Koh, D. R. Abujetas, J. A. Sánchez-Gil, R. Paniagua-Domínguez, H. V. Demir, and A. I. Kuznetsov, *Nano Lett.* **20**, 6005 (2020).
- [13] V. Mylnikov, S. T. Ha, Z. Pan, V. Valuckas, R. Paniagua-Domínguez, H. V. Demir, and A. I. Kuznetsov, *ACS Nano* **14**, 7338 (2020).
- [14] A. Tripathi, H.-R. Kim, P. Tonkaev, S.-J. Lee, S. V. Makarov, S. S. Kruk, M. V. Rybin, H.-G. Park, and Y. Kivshar, *Nano Lett.* **21**, 6563 (2021).
- [15] Y. Yu, A. Sakanas, A. R. Zali, E. Semenova, K. Yvind, and J. Mørk, *Nat. Photonics* **15**, 758 (2021).
- [16] M.-S. Hwang, H.-C. Lee, K.-H. Kim, K.-Y. Jeong, S.-H. Kwon, K. Koshelev, Y. Kivshar, and H.-G. Park, *Nat. Commun.* **12**, 1 (2021).
- [17] L. Carletti, S. S. Kruk, A. A. Bogdanov, C. De Angelis, and Y. Kivshar, *Phys. Rev. Res.* **1**, 023016 (2019).
- [18] L. Xu, K. Zangeneh Kamali, L. Huang, M. Rahmani, A. Smirnov, R. Camacho-Morales, Y. Ma, G. Zhang, M. Woolley, D. Neshev *et al.*, *Adv. Sci.* **6**, 1802119 (2019).
- [19] T. Ning, X. Li, Y. Zhao, L. Yin, Y. Huo, L. Zhao, and Q. Yue, *Opt. Express* **28**, 34024 (2020).
- [20] C. Fang, Q. Yang, Q. Yuan, X. Gan, J. Zhao, Y. Shao, Y. Liu, G. Han, Y. Hao *et al.*, *Opto-Electron. Adv.* **4**, 200030 (2021).
- [21] G. Zograf, K. Koshelev, A. Zalogina, V. Korolev, R. Hollinger, D.-Y. Choi, M. Zuerch, C. Spielmann, B. Luther-Davies, D. Kartashov *et al.*, *ACS Photonics* **9**, 567 (2022).
- [22] A. Tittl, A. Leitis, M. Liu, F. Yesilkoy, D.-Y. Choi, D. N. Neshev, Y. S. Kivshar, and H. Altug, *Science* **360**, 1105 (2018).
- [23] F. Yesilkoy, E. R. Arvelo, Y. Jahani, M. Liu, A. Tittl, V. Cevher, Y. Kivshar, and H. Altug, *Nat. Photonics* **13**, 390 (2019).
- [24] D. N. Maksimov, V. S. Gerasimov, S. Romano, and S. P. Polyutov, *Opt. Express* **28**, 38907 (2020).
- [25] I. Yusupov, D. Filonov, A. Bogdanov, P. Ginzburg, M. V. Rybin, and A. Slobozhanyuk, *Appl. Phys. Lett.* **119**, 193504 (2021).
- [26] Y. Jahani, E. R. Arvelo, F. Yesilkoy, K. Koshelev, C. Cianciaruso, M. De Palma, Y. Kivshar, and H. Altug, *Nat. Commun.* **12**, 3246 (2021).
- [27] A. Burin, H. Cao, G. Schatz, and M. Ratner, *J. Opt. Soc. Am. B* **21**, 121 (2004).
- [28] A. Asenjo-Garcia, M. Moreno-Cardoner, A. Albrecht, H. J. Kimble, and D. E. Chang, *Phys. Rev. X* **7**, 031024 (2017).
- [29] D. F. Kornovan, R. S. Savelev, Y. Kivshar, and M. I. Petrov, *ACS Photonics* **8**, 3627 (2021).
- [30] E. Bulgakov, A. Pilipchuk, and A. Sadreev, *Phys. Rev. B* **106**, 075304 (2022).
- [31] K. Koshelev, S. Lepeshov, M. Liu, A. Bogdanov, and Y. Kivshar, *Phys. Rev. Lett.* **121**, 193903 (2018).
- [32] See Supplemental Material at <http://link.aps.org/supplemental/10.1103/PhysRevB.107.195108> for multipole decomposition, mode amplitudes according to the effective Hamiltonian and configuration description.
- [33] A. A. Dmitriev and M. V. Rybin, *Phys. Rev. A* **99**, 063837 (2019).